Impact of irradiation damage recovery during transportation on the subsequent room temperature tensile behavior of irradiated zirconium alloys

B. Bourdiliau, F. Onimus, C. Cappelaere, V. Pivetaud, P. Bouffioux, V. Chabretou, A. Miquet

B. Bourdiliau, F. Onimus, C. Cappelaere, V. Pivetaud, P. Bouffioux, V. Chabretou, A. Miquet (2010) Impact of the irradiation damage recovery during transportation on the subsequent room temperature tensile behavior of irradiated zirconium alloys, Journal of ASTM International, Vol. 7, No. 9 (16th International Symposium on Zirconium in the Nuclear Industry, 9th May 2010 – 13th May 2010, Chengdu, Sichuan Province, China).

Symposium: *16th International Symposium on Zirconium in the Nuclear Industry, 9th May 2010 – 13th May 2010, Chengdu, Sichuan Province, China*

Paper Title: Impact of the irradiation damage recovery during transportation on the subsequent room temperature tensile behavior of irradiated zirconium alloys

Authors: B.BOURDILIAU[1], F.ONIMUS[2], C. CAPPELAERE[1], V. PIVETAUD[1], P. BOUFFIOUX[3], V. CHABRETOU[4], A. MIQUET[5]

[1], *CEA/DEN/DMN/SEMI, CEA-Saclay, 91191 Gif-sur-Yvette, France*
[2], *CEA/DEN/DMN/SRMA, CEA-Saclay, 91191 Gif-sur-Yvette, FRANCE*
[3], *EDF/R&D Les Renardières, Ecuelles. 77818 MORET SUR LOING CEDEX, FRANCE*
[4], *AREVA, AREVA NP SAS, 10 Rue Juliette Récamier 69456 LYON CEDEX 6, FRANCE*
[5], *EDF/SEPTEN 12-14 Avenue Dutriévoz, 69628 Villeurbanne, FRANCE*

Abstract

Zirconium alloys are commonly used in Pressurized Water Reactor as fuel rod cladding tubes. After irradiation and cooling in pool, the Spent Nuclear Fuel Assemblies are either transported for wet storage to a devoted site or loaded in suitable casks for dry storage on Nuclear Power Plant site. During dry transportation or at the beginning of dry storage, at temperatures around 400°C, the cladding experiences a creep deformation under the hoop stress induced by the internal pressure of the fuel rod. During creep a recovery of the radiation damage can occur that can affect the subsequent mechanical properties.

The mechanical behavior of the cladding has been investigated in laboratory on two neutron irradiated cladding materials: fully recrystallized Zr-1%Nb and stress relieved Zircaloy-4. Creep tests under internal pressure were conducted at 400°C and 420°C. After depressurization and cooling, ring tensile tests were carried out at room temperature. In addition, Transmission Electron Microscopy observations have been performed after testing.

The post-creep mechanical response exhibited a decrease of the strength compared to the as-irradiated material. This decrease is associated with a significant recovery of the ductility, which becomes close to the ductility of the unirradiated material. The Transmission Electron Microscopy examinations, especially conducted on recrystallized Zr-1%Nb ring samples, revealed that the radiation defects have been annealed. It was also observed that, as for the unirradiated material, the deformation occurred homogeneously throughout the grains. No dislocation channel was indeed observed contrary to the as-irradiated material. These observations explain the recovery of the strength and of the ductility after post-irradiation creep that may occur during dry transportation or at the beginning of dry storage.

Keywords

Ring tensile test, Transmission Electron Microscopy, internal pressure creep test, heat treatment, deformation mechanisms, Zy-4, Zr-1%Nb, spent nuclear fuel, transportation.

1. Introduction

Zirconium alloys are commonly used in Pressurized Water Reactors (PWR) as fuel cladding tubes. After irradiation and cooling in pool, the Spent Nuclear Fuel Assemblies (SNFA) are either transported for wet storage to a devoted site or loaded in suitable casks for dry storage on Nuclear Power Plant site. During dry shipment or at the beginning of dry storage, the cladding experiences creep deformation due both to the fuel rod inner pressure of the fission gas and the significant temperature induced by the residual power of the fuel [1]. In order to guarantee the integrity of the cladding when retrieving the SNFA both after shipment and storage, it is essential to obtain a good knowledge of the effects of the transportation on the room temperature mechanical properties of the materials.

It has been shown in a previous study [2] that during a creep test, representative of transportation conditions, recovery of the radiation damage occurs in addition to the creep deformation mechanisms. It has also been shown [2, 3] that the recovery of the irradiation damage is associated with the recovery of the hardening induced by irradiation, as demonstrated by Transmission Electron Microscopy (TEM) observations and microhardness tests carried out at room temperature after heat treatments on as-irradiated zirconium alloys.

In order to have a better knowledge and understanding of the effect of post-irradiation creep testing on the subsequent room temperature mechanical properties of zirconium alloys, a thorough study has been achieved. This study is based first on microhardness tests performed on the neutron irradiated zirconium alloys after creep testing but also on tensile tests carried on at room temperature on ring specimens which were machined out of specimens after creep testing. In addition, on some of the tensile tests specimens, TEM observations have been performed after testing in order to obtain a better understanding of the deformation mechanisms in such testing conditions. The experimental results are presented in the first part

of the paper. Then, in the last part, the results are discussed and interpreted in terms of microstructure and deformation mechanisms.

2. Materials and experimental details

2.1. Materials studied

Two cladding materials have been studied: the stress relieved Zircaloy-4 and a recrystallized annealed Zr-1%Nb alloy. The chemical composition of the two alloys are given in Table 1. The materials have been irradiated from four up to six PWR cycles and then cut and defueled in order to perform mechanical tests.

Table 1: Chemical composition of the alloys (wt%)

Alloy	Metallurgical state	Sn	Fe	Cr	Nb	O	Zr
Zy-4	Stress-relieved	1.4	0.2	0.10	-	0.125	Bal.
Zr-1%Nb	Recrystallized	-	0.02	-	1.0	0.125	Bal.

2.2. Mechanical testing

2.2.1 Creep specimens

Four stress-relieved Zy-4 specimens irradiated up to four PWR cycles have been tested under internal pressure during creep tests with an applied stress of 130 MPa and at temperatures from 380 up to 420°C, and during 1000 to 17000 hours. The creep tests were performed either in an internal pressure creep furnace with controlled internal gas pressure (hereafter called Controlled Gas Pressure, CGP) or as pre-pressurized samples (with internal gas pressure) in a furnace (called LTC, Long Term Creep). The controlled internal pressure creep test (CGP) is performed at constant pressure and, at the end of the test, the specimen is depressurized before cooling. For the long term creep (LTC) test, the stress in the pre-pressurized specimen

remains constant and gradually falls during cooling. The creep test conditions are given in Table 2.

Three recrystallized Zr-1%Nb specimens irradiated from four up to five PWR cycles have also been tested under internal pressure creep test (in CGP or LTC conditions) with an applied stress of 130 MPa and at temperatures from 400 up to 420°C during 900 up to 3300 hours. The creep test conditions are given in Table 3 as well as the creep strains at the end of the tests.

Table 2: Testing conditions for the creep tests performed on the Zy-4 specimens. References of the tensile tests specimens performed at room temperature are given in the last column. The following acronyms stand for: LTC: Long-Term Creep, CGP: Controlled Gas Pressure.

Creep specimen	Creep test type	Creep temperature, °C	Creep stress, MPa	Creep duration, hours	Tensile specimen
Zy4-1 4 cycles	LTC	420	130	4974	Zy4-1a Zy4-1b
Zy4-2 4 cycles	CGP	420	130	1077	Zy4-2a Zy4-2b
Zy4-3 4 cycles	LTC	380	130	14994	Zy4-3a Zy4-3b
Zy4-4 4 cycles	LTC	400	130	17071	Zy4-4
Zy4-5 As-irradiated 4 cycles	-	-	-	-	Zy4-5a Zy4-5b
Zy4-6 Non-irradiated	-	-	-	-	Zy4-6a Zy4-6b

Table 3: Testing conditions for the creep tests performed on the Zr-1%Nb specimens. References of the tensile tests specimens performed at room temperature are given in the last column. The following acronyms stand for: LTC: Long-Term Creep, CGP: Controlled Gas Pressure. The star (*) indicates the interrupted tests at UTS for TEM observations after testing.

Creep sample	Creep test type	Creep temperature °C	Creep stress, MPa	Creep duration, hours	Tensile specimen
ZrNb-1 5 cycles	LTC	400	130	3301	ZrNb-1a ZrNb-1b
ZrNb-2 4 cycles	CGP	400	130	984	ZrNb-2a* ZrNb-2b
ZrNb-3 4 cycles	CGP	420	130	912	ZrNb-3a* ZrNb-3b
ZrNb-4 As irradiated 6 cycles	-	-	-	-	ZrNb-4a* ZrNb-4b
ZrNb-5 Non irradiated	-	-	-	-	ZrNb-5a ZrNb-5b

2.2.2 Hardness measurements

After the creep tests, 10 mm long sections of the specimens have been cut, embedded into a resin and then mechanically polished in hot cell. Vickers microhardness experiments have been carried out using 200 g load along the z-direction of the tube (on the r-θ cross section of the tube). In order to provide correct statistical results, ten hardness measures are performed for each sample at room temperature.

2.2.3 Tensile ring specimens

Tensile ring specimens have also been spark machined out of the cladding specimens (both Zy-4 and Zr-1%Nb) after creep tests. The rings, cut out in the transverse section of a PWR cladding, were 3 mm long and 2 mm wide in the gauge length. The Fig. 1 shows an example of a tensile ring machined out of a long term creep specimen. Two rings were cut out from a single creep specimen (except the Zy4-4 specimen), from each side of its symetry axis. Moreover, two as-irradiated specimens, and two unirradiated specimens were machined for both materials. The rings have then been tested on an electromechanical tensile machine fitted with a LVDT sensor and a 50 kN load cell. The specimen was placed on its mandrel so that the sample legs were centered over the loading axis. The tensile test was displacement-controlled. All the tests were performed at room temperature with a strain rate of 3×10^{-4} s^{-1}. Several tensile conventional properties are deduced from the tensile curves. The engineering stress is given as a function of the engineering strain: the Yield Stress (YS, stress at 0.2 % plastic strain offset given in MPa), the Ultimate Tensile Strength (UTS, stress corresponding to the maximum force given in MPa), Uniform Elongation (UE, plastic strain measured at maximum force, in %), Total Elongation (TE, plastic strain at fracture, in %). The stress – strain curves have been corrected from the overall testing machine stiffness, which is the result of the elastic deformation in the load line device and the mandrel stiffness. A Young modulus of E = 100 GPa at room temperature has been chosen in agreement with the values given by Northwood et al. [4].

Pictures of the ring specimens after testing were systematically taken. Some of these pictures are shown hereafter.

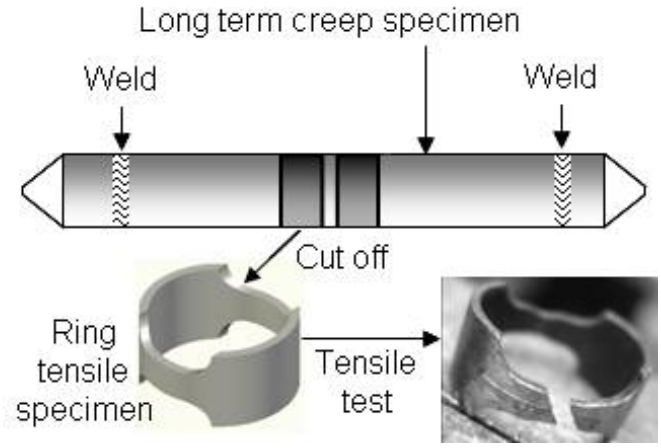

Figure 1: Example of a tensile ring machined out of a long term creep specimen. The second ring was prepared the same way.

Concerning the Zr-1%Nb alloy, the non irradiated specimens were 88 ppm gaseous hydrided in order to simulate the hydriding which occurs in-reactor and therefore only measure the effect of irradiation, uncorrelated from the hydriding effect. In addition, in the case of the Zr-1%Nb alloy, under each test condition, one ring was tested up to failure and a second one was stopped at UTS (indicated with a star (*) in Table 3). In these specimens, thin foils have been taken in order to perform TEM observations of the as-deformed microstructure.

2.3. Transmission Electron Microscopy

Transmission Electron Microscopy (TEM) observations were carried out on neutron irradiated Zr-1%Nb previously tested only until the maximum load. The tests conditions of these samples are given in Table 3.

After testing, the legs of ring specimens have been cut and mechanically polished in hot cell. Thin foils have been taken from the polished legs and electro-polished in a glove box.

The TEM observations have then been performed on a Philips EM 430 operating at 300 keV accelerating voltage. The study has been performed using double tilt sample holder, conventional imaging of crystalline defects and diffraction pattern indexing.

3. Experimental results

3.1. Mechanical Tests

3.1.1 Zy-4 specimens

The engineering stress - strain curves corresponding to the tests performed on Zy-4 are shown on Fig. 2. Tensile conventional properties deduced from the stress – strain curves are given in Table 4.

Table 4: Tensile conventional mechanical properties deduced from the engineering stress – strain curves obtained for Zy-4 specimens (at room temperature)

Ring sample	Creep temperature - duration	YS (MPa)	UTS (MPa)	UE (%)	TE (%)
Zy4-1a	420°C - 4974 h	676	731	1.71	17.97
Zy4-1b		686	743	1.69	17.32
Zy4-2a	420°C - 1077 h	719	787	2.05	18.80
Zy4-2b		688	764	2.02	18.89
Zy4-3a	380°C - 14994 h	722	778	1.94	17.31
Zy4-3b		722	788	1.49	15.89
Zy4-4	400°C - 17071 h	674	745	2.16	17.59
Zy4-5a	As-irradiated	916	966	0.84	9.89
Zy4-5b		940	989	0.87	8.68
Zy4-6a	Non irradiated	693	763	2.28	25.70
Zy4-6b		689	763	2.69	26.74

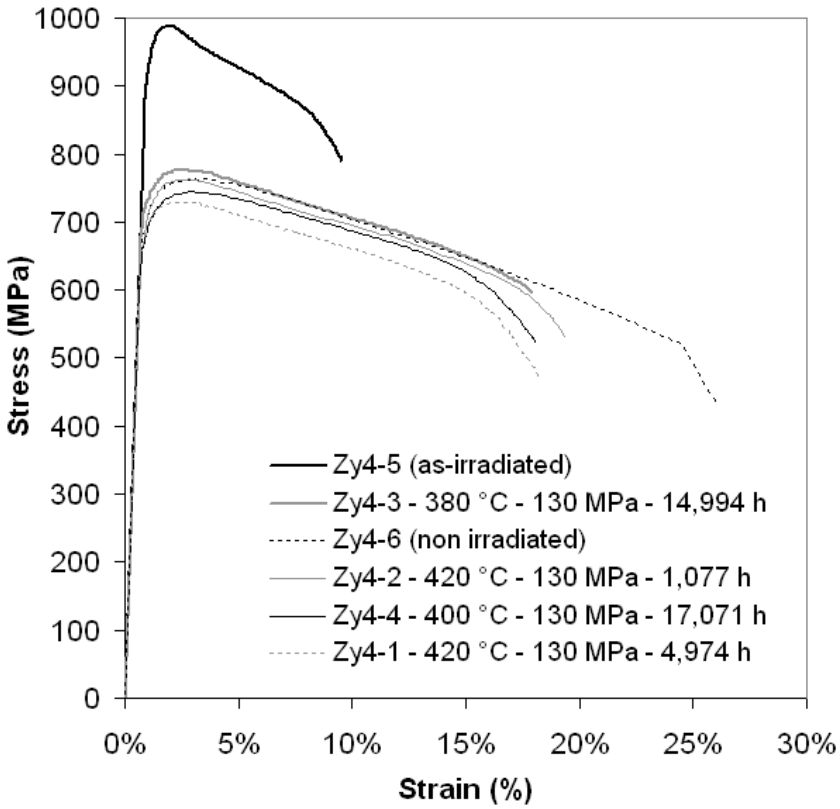

Figure 2: Engineering stress - strain curves obtained during ring tensile tests performed at room temperature on Zy-4 specimens after neutron irradiation and creep test. Tensile tests on non irradiated and as-irradiated Zy-4 specimens are also given.

When comparing the non irradiated Zy-4 specimens and the as-irradiated specimens, Fig. 2 and Table 4 demonstrate that neutron radiation leads to a strong hardening (increase of the YS and UTS values) as well as to a reduction of the macroscopic ductility (decrease of the UE and TE values).

After creep, it can be seen on Fig. 2 and on Table 4 that the YS as well as the UTS values have decreased compared to the as-irradiated behavior. It is also shown that after the creep test, the UE as well as the TE values have increased proving that the creep test leads to a recovery of the ductility of the material.

However, it can be noticed on Fig. 2 and on Table 4 that after creep tests the room temperature tensile behavior remains different from the non-irradiated mechanical behavior. Indeed, the UE and TE values remain systematically lower than the values measured for the non-irradiated Zy-4, proving that the macroscopic ductility of the material was not fully recovered even after 4974 hours at 420°C (specimen Zy4-1) or after 17071 hours at 400°C. On the other hand, the strength (YS and UTS) of the material can be fully recovered after creep test and can even become lower than the YS and UTS values measured on the non irradiated material.

It can also be noticed that when the creep temperature increases from 380°C up to 420°C, the strength (YS and UTS) tends to a slight decrease. Increasing the duration of the creep test leads also to a slight decrease of the strength after creep. Concerning the UE and TE values, no obvious evolution with creep test temperature and duration can be observed.

The pictures of the ring specimens after tensile tests on the as-irradiated Zy-4 and on the Zy-4 after creep test (Zy4-2) show that the failure occurs only on one leg by shearing and propagation of a crack making a 45° angle with the tensile axis, which confirms a ductile fracture. Nevertheless, the necking of the gauge length of the ring remains limited for both specimens (Fig. 3). It is worth noticing that the as-irradiated specimen and the specimen after post-irradiation creep test exhibit similar fracture morphology.

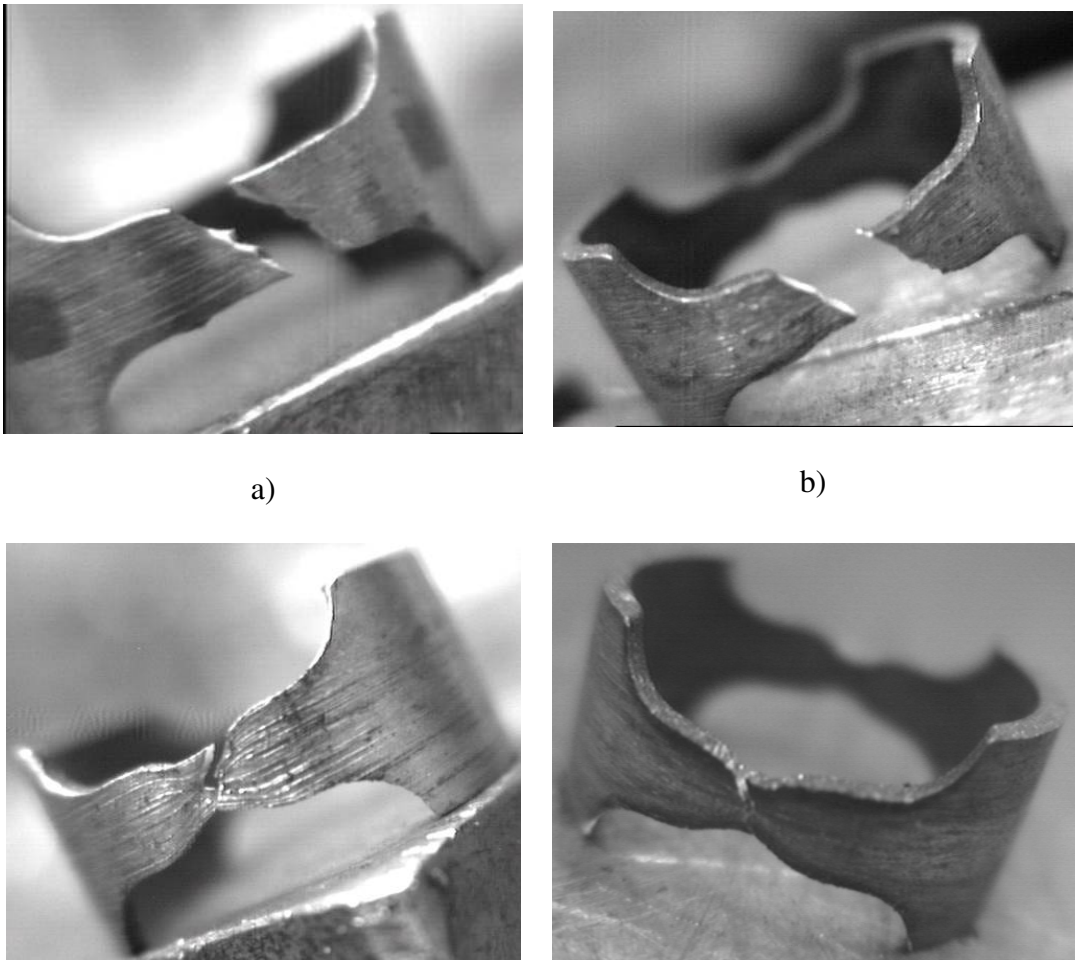

a) b)

c) d)

Figure 3: Pictures of the ring tensile test specimens after failure for : a) as-irradiated Zy-4 specimen (Zy4-5a), b) creep tested Zy-4 specimen (Zy4-2a), c) as-irradiated Zr-1%Nb specimen (ZrNb-4b), d) creep tested Zr-1%Nb specimen (ZrNb-1b).

3.1.2 Zr-1%Nb specimens

The engineering stress - strain curves corresponding to the tests performed on the Zr-1%Nb specimens are shown on Fig. 4 and the conventional tensile properties are given in Table 5.

Table 5: Mechanical properties obtained for Zr-1%Nb specimens. The star (*) indicates the tests interrupted at UTS in order to provide samples for TEM observations.

Ring sample	Creep temperature - duration	YS (MPa)	UTS (MPa)	UE (%)	TE (%)	UTS-YS (MPa)
ZrNb-1a	400°C – 3301 h	470	555	5.01	27.17	85
ZrNb-1b		484	558	3.91	29.57	74
ZrNb-2a	400°C – 984 h	515	568	2.43 (*)	-	53
ZrNb-2b		525	577	2.63	27.59	52
ZrNb-3a	420°C – 912 h	475	544	5.16 (*)	-	69
ZrNb-3b		477	536	4.76	30.95	59
ZrNb-4a	As-irradiated	734	741	0.41 (*)	-	7
ZrNb-4b		721	734	0.49	30.88	13
ZrNb-5a	Non irradiated hydrided	460	498	9.26	42.74	38
ZrNb-5b		460	487	6.96	43.07	27

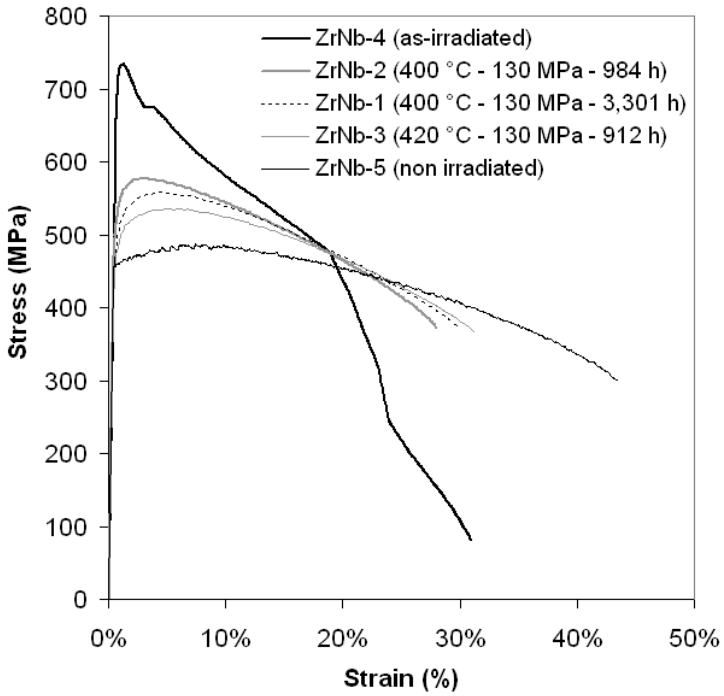

Figure 4: Engineering stress - strain curves obtained during ring tensile tests performed at room temperature on Zr-1%Nb specimens after neutron irradiation and creep test. Tensile tests on non irradiated and as-irradiated Zr-1%Nb specimens are also provided.

Fig. 4 and Table 5 show that, such as for Zy-4 specimens, neutron irradiation leads to a strong hardening, as shown by the increase of the YS and UTS values when comparing the non irradiated and the as-irradiated specimens, and to a reduction of the macroscopic ductility (decrease of the UE and TE values). On the tensile curve of the as-irradiated ring tested up to failure, we can see a load drop just after the UTS. In addition, the tensile curve exhibits a sudden acceleration of the load decrease during the necking.

After post-irradiation creep, it can be seen on Fig. 4 and on Table 5 that the YS as well as the UTS values of the Zr-1%Nb specimens have decreased compared to the as-irradiated behavior, proving that a recovery of the radiation hardening has occurred during the creep test. It is also shown that, after the creep test, the UE values have increased proving that the post-irradiation creep test leads to a recovery of the ductility of the material.

However, it can be noticed, when comparing the behavior after post irradiation creep to the behavior before irradiation, that YS and UTS values after creep are still higher than the values measured before irradiation. The macroscopic ductility also appears to be only partially recovered after creep: the UE and TE values remain lower than the values measured before irradiation. It is also worth noticing that the strain hardening behavior after post-irradiation creep is also very different from the strain hardening behavior before irradiation. Indeed, on the non irradiated Zr-1%Nb specimens, the strain hardening rate is low just after the onset of plastic flow and decreases slowly until reaching the maximum load whereas in the case of the Zr-1%Nb after post-irradiation creep, the strain hardening remains high at the onset of plastic flow and decreases more quickly until reaching the maximum load. This change of strain hardening behavior due to the post-irradiation creep test can be characterized by the difference between UTS and YS values. Table 5 shows, indeed, that the difference between UTS and YS values after post-irradiation creep is nearly twice higher than the difference

between the UTS and YS values measured on the non irradiated specimens. This proves that the strain hardening after post irradiation creep is higher than the strain hardening before irradiation.

It can also be noticed that when the creep temperature or the creep duration increase, the strength (YS and UTS values) slightly decreases and the ductility (UE and TE values) increases.

The pictures taken after the tensile test (Fig. 3) show that both the as-irradiated Zr-1%Nb specimen and the Zr-1%Nb specimen tested after post-irradiation creep show a significant necking. Strong shearing is observed as the crack shows a 45° angle with the tensile axis. The crack is close to 45° on one side of the reduced area, and close to 135° on the other side, due to a change of the crack propagation direction at the reduced area center. It is worth noticing that both specimens shown on Fig. 3 exhibit the same fracture morphology

3.2 Microhardness measurements

3.2.1 Zy-4 specimens

Table 6 displays the Vickers microhardness obtained on the Zy-4 specimens. Hardness values and measured UTS values were compared.

It can be seen on Table 6, when comparing the as-irradiated to the non irradiated Zy-4 specimens, that irradiation leads to a significant increase of the hardness linked to the radiation induced hardening observed during the tensile test. After creep test, the hardness value decreases strongly because of the recovery of the radiation induced hardening. It can be seen that, as for the YS or the UTS values, depending on the post-irradiation creep conditions, the hardness of the Zy-4 specimens can even become lower than the hardness of the non irradiated Zy-4 specimen.

Table 6: Microhardness values measured after post-irradiation creep tests on Zy-4 specimens compared to UTS values measured during tensile tests after post-irradiation creep tests.

Tensile sample	Creep temperature - duration	UTS (MPa)	Microhardness (HV)
Zy4-1a	420°C - 4974 h	731	235 ± 5
Zy4-1b	420°C - 4974 h	743	
Zy4-2a	420°C - 1077 h	787	244 ± 3
Zy4-2b	420°C - 1077 h	764	
Zy4-5a	As-irradiated	966	300 ± 8
Zy4-5b	As-irradiated	989	
Zy4-6a	Non irradiated	763	244 ± 3
Zy4-6b	Non irradiated	763	

The hardness values measured after post-irradiation creep test are also compared on the Fig. 5 to the hardness evolution obtained in a previous study [2] after post-irradiation heat treatments performed on Zy-4 at 350°C, 400°C and 420°C. The empirical recovery law proposed in [5, 6] and adjusted in [2] is also shown on Fig. 5. The recovered fraction of hardness, *f*, is defined in Eq. 1.

$$f = \frac{H_v^{AsI} - H_v(t)}{H_v^{AsI} - H_v^{NI}} \qquad (1)$$

The values H_v^{AsI}, H_v^{NI} and $H_v(t)$ used in Eq. 1 are respectively the as-irradiated hardness of the material, the non-irradiated hardness of the material and the current hardness of the material all along the heat treatment. According to Dollins [6], the hardness recovered fraction follows a chemical kinetics empirical law, expressed in Eq. 2.

$$\frac{df}{dt} = k(1-f)^n \qquad (2)$$

In Eq. 2, the coefficient k can be written as $k = k_0 \exp(-Q/k_B T)$ where k_B is the Boltzmann constant, T is the temperature of the heat treatment, Q the activation energy of the recovery and k_0 a coefficient. The fitted values are n = 2.3, k_o = 1.8×10^8 s^{-1} and Q = 1.800 eV [2]. As pointed out in [2], since in the empirical law the reference hardness value is the hardness before irradiation, the empirical law chosen here is therefore not able to reproduce the decrease of the hardness below its value before irradiation.

It can be seen on Fig. 5 that the hardness values measured after post-irradiation creep tests performed on Zy-4 specimens at 420°C during 1077 hours and 4974 hours are in good agreement with the hardness measured after post-irradiation heat treatment performed at 420°C for similar duration showing that the effect of post-irradiation creep on the hardness of Zy-4 is the same as a post-irradiation heat treatment.

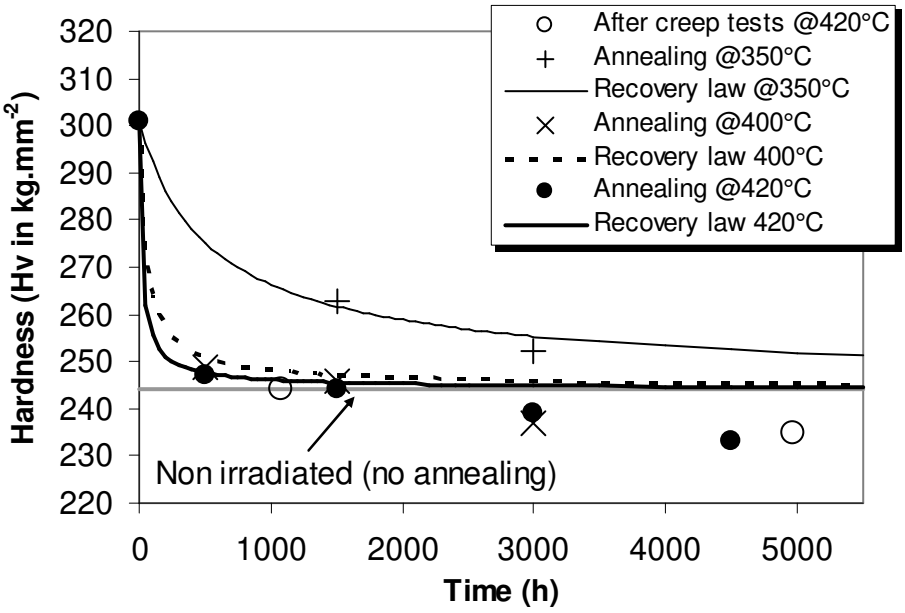

Figure 5: Comparison between the hardness evolution after post-irradiation creep tests and post-irradiation heat treatments performed on Zy-4 specimens at 350°C, 400°C and 420°C. The recovery law obtained in [2] is also shown.

3.2.2 Zr-1%Nb Specimens

The hardness values obtained on the Zr-1%Nb specimens after post-irradiation creep performed at 400°C are given in Table 7 and compared to the UTS values. As for the Zy-4 specimens, the hardness values of the Zr-1%Nb specimens follow the same evolution as the YS and UTS values. It can be seen on Table 7 that irradiation induces a strong hardening when comparing the hardness of the as-irradiated Zr-1%Nb and the hardness of the non irradiated Zr-1%Nb specimens. As for the YS and UTS values, it can be seen that after post-irradiation creep the hardness decreases due to the recovery of the radiation induced hardening. However, it can be observed that the hardness values after post-irradiation creep of Zr-1%Nb specimens always remain higher than before irradiation.

The hardness values measured after post-irradiation creep tests performed at 400°C were also compared on the Fig. 6 to the hardness evolution obtained in a previous study [2] after post-irradiation heat treatments performed on a Zr-1%Nb alloy at 350°C, 400°C and 450°C. The empirical recovery law adjusted in [2] is also shown on Fig. 6. The values of the fitting parameters are n = 3.1, $k_o = 3.8\times10^2$ s^{-1} and Q = 1.075 eV.

It can be observed on Fig. 6 that after post-irradiation creep performed at 400°C during 984 or 3301 hours, the hardness of the Zr-1%Nb specimens remains higher than the hardness measured after a post-irradiation heat treatment at 400°C lasting only 500 hours. This proves that in the case of the Zr-1%Nb specimens, post irradiation creep and heat treatment have different effects on the hardness.

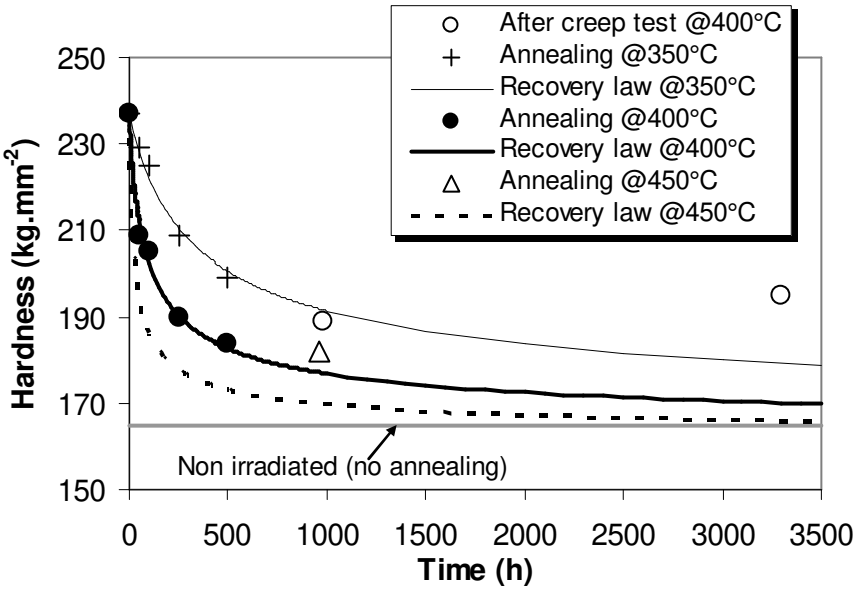

Figure 6: Comparison between the hardness evolution after post-irradiation creep tests and post-irradiation heat treatments performed on Zr-1%Nb specimens at 350°C, 400°C and 420°C. The recovery law obtained in [2] is also shown.

Table 7: Microhardness values measured after post-irradiation creep tests on Zr-1%Nb specimens compared to UTS values measured during tensile tests after post-irradiation creep tests.

Tensile sample		UTS (MPa)	Microhardness (HV)
ZrNb-1a	400°C – 3301 h	555	
			195 ± 5
ZrNb-1b	400°C – 3301 h	558	
ZrNb-2a	400°C – 984 h	568	
			189 ± 5
ZrNb-2b	400°C – 984 h	577	
ZrNb-4b	As-irradiated	734	
			237 ± 6
ZrNb-4a	As-irradiated	741	
ZrNb-5d	Non irradiated	487	
			165 ± 5
ZrNb-5c	Non irradiated	498	

3.2.3 Correlation between hardness and UTS values

Tables 6 and 7 show that the hardness and the UTS values follow the same evolution for Zy-4 and Zr-1%Nb specimens. The change in UTS (with respect to the non irradiated material) can therefore be plotted in Fig. 7 as a function of the change in hardness (with respect to the non irradiated material) for both alloys. It can be observed on Fig. 7 that there is a linear relationship for all specimens between the change in UTS measured in the hoop direction and provided by the ring tensile tests and the change in Vickers hardness measured on the r-θ cross section of the tube. The proportionality coefficient is: $\Delta UTS = 3.485 \Delta H_v$ with ΔUTS

in MPa and ΔH_v in kg.mm^{-2}. This analysis is in agreement with the relationship obtained by Busby et al. [8] between hardness and yield stress in irradiated austenitic and ferritic steels. The good correlation obtained between UTS values and hardness values confirm that the two techniques provide a coherent quantification of the recovery state of the material after post-irradiation creep testing. In the following, these techniques are both used and compared to the TEM obsvervations.

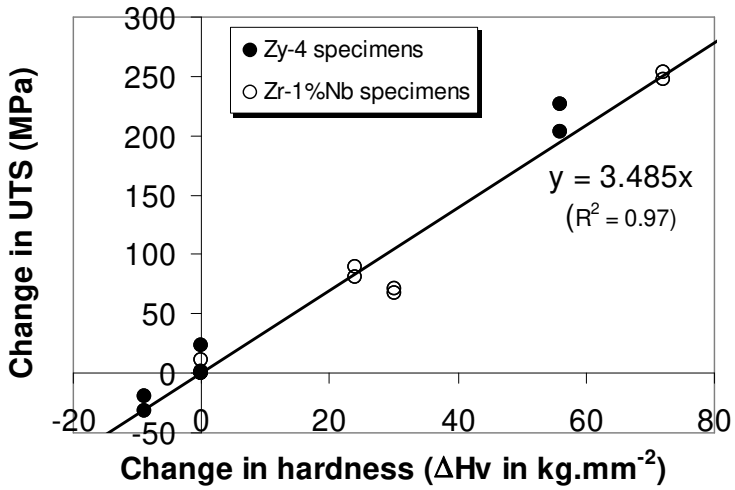

Figure 7: Correlation between the change in UTS and the change in hardness for both Zy-4 and Zr-1%Nb specimens.

3.3. Results of the TEM observations on Zr-1%Nb samples

3.3.1 As-irradiated sample observed after tensile test

TEM observations have been performed on the as-irradiated sample after tensile testing. TEM pictures of the microstructure obtained after deformation are given in Fig. 8. It can be observed that the microstructure exhibits cleared bands or so-called dislocation channels in numerous grains. The channeling plane has been analyzed using the method described in [8, 9]. It can be seen on Fig. 8(a) that the channeling plane corresponds to the basal plane. Deviation of the basal channels on the pyramidal plane can also be observed on Fig. 8(a).

On the other hand, it can be seen that in several grains (Fig. 8(b), 8(c), 8(d)) the observed channels do not correspond to the basal plane. Indeed, the channels can be observed even when the basal plane is nearly perpendicular to the electron beam. The channeling planes have been analyzed and correspond to the prismatic planes. Moreover it appears that contrarily to the basal channels which are only clearly observed when the basal plane nearly contains the electron beam, the prismatic channels can be observed for a wide tilt angle range, even when the electron beam is far from the prismatic plane. This can lead to a more ambiguous determination of the channeling plane.

Since the orientation of the tensile axis is known on the thin foil it is possible to compute the Schmid factors of the various slip systems for each grain observed. The basal and prismatic Schmid factors of the grains observed on Fig. 8 are given in Table 8. It can be seen on Table 8 that, when the basal plane is well orientated for slip (high basal Schmid factor), basal channeling occurs. On the other hand, when the basal plane is not well orientated for slip (low basal Schmid factor) prismatic channeling occurs.

Table 8: Basal and prismatic Schmid factors for the four grains observed by TEM given Fig. 8. For basal slip the maximum basal Schmid factor is always given. For prismatic slip the prismatic Schmid factor corresponding to the activated slip system is given, when only basal channels are observed the maximum prismatic Schmid factor is given.

Grain observed	Maximum basal Schmid factor	Prismatic Schmid factor	Channeling plane observed
Grain 1 on Fig. 8(a)	0.4	0.12	Basal
Grain 2 on Fig. 8(b)	0.29	0.45	Prismatic
Grain 3 on Fig. 8(c)	0.16	0.47	Prismatic
Grain 4 on Fig. 8(d)	0.26	0.45	Prismatic

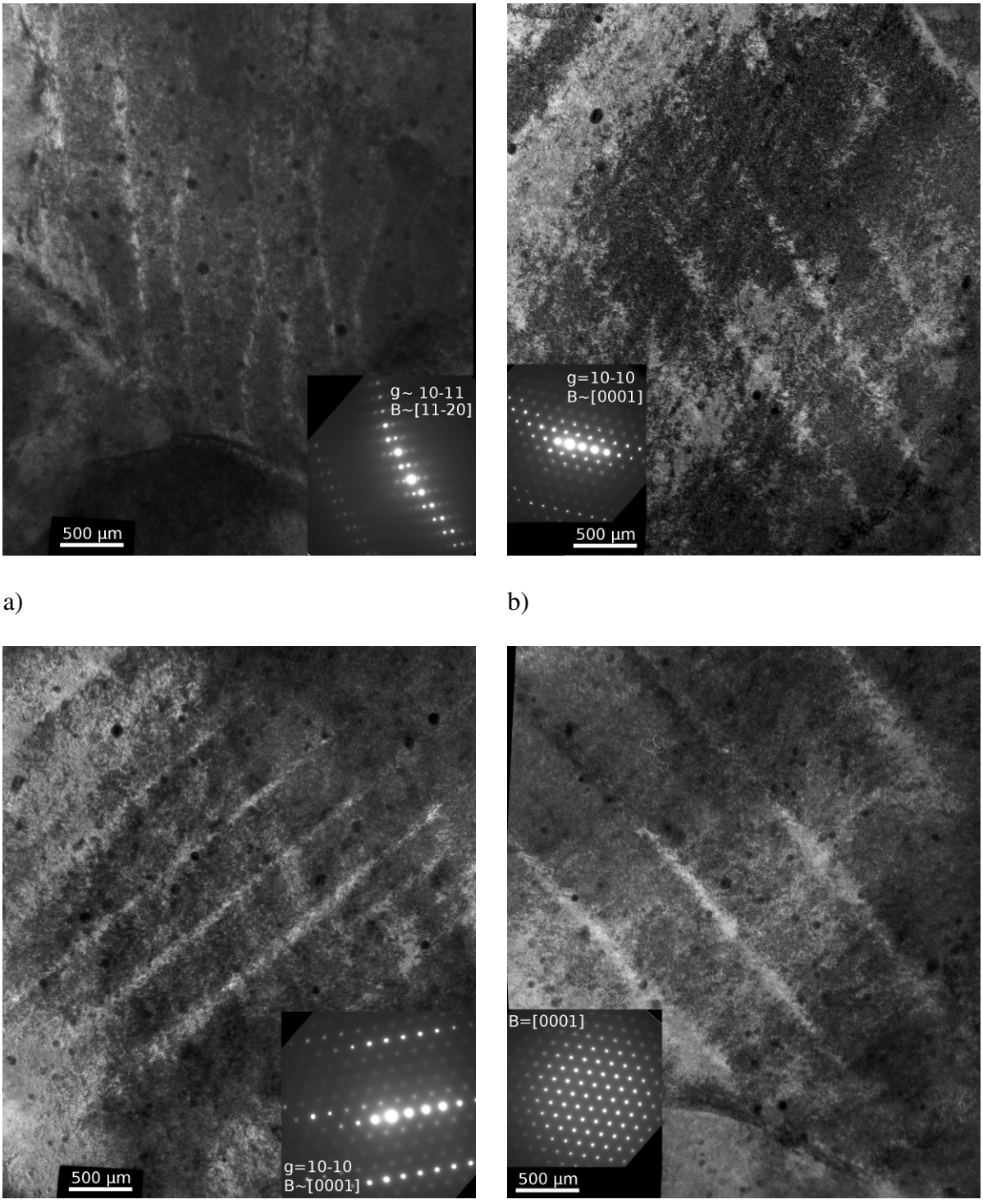

Figure 8: Pictures of the ZrNb-4a specimen microstructure: the channels appear as clear bands. a) basal channels in grain 1 observed with the electron beam close to the basal plane

($B \approx [1\bar{1}20]$) using the diffraction vector $g = 20\bar{2}1$, b) and c) prismatic channels in grain 2 and 3 observed with the electron beam close to the <c> axis ($B \approx [0001]$) using the diffraction vector $g = 10\bar{1}0$, d) prismatic channels in grain 4 observed with the electron beam close to the <c> axis ($B \approx [0001]$). The picture has been observed in two beams condition close to the [0001] zone axis diffraction pattern shown on the picture.

3.3.2 Samples observed after tensile tests following creep tests performed at 400°C and 420°C with 130 MPa

TEM observations have been performed after room temperature tensile tests following post-irradiation creep tests at 400°C and 420°C under 130 MPa in internal pressure. It can be seen on Fig. 9 that the dislocation density observed after tensile tests is significant and that the dislocations appear to be tangled. No dislocation channel can be observed, on the contrary of what occurs for the as-irradiated specimen, and the deformation is distributed homogeneously within the grains. It can also be noticed on Fig. 9 that the microstructures observed for the two creep tests conditions (400°C and 420°C) are very similar.

On the Fig. 9(a), where the grain is observed with the electron beam close to the <c> axis, two linear dislocation systems are clearly observed at 120° from each other. This shows that in that grain, the prismatic slip is mainly activated. On the Fig. 10(a) and 10(b) the same area is shown using two different diffraction conditions. Nb-rich precipitates under the shape of needles are clearly observed on Fig. 10(b) without any contrast coming from the loops or the dislocations. The microstructure (size and density) of the needle-like precipitates appear to be similar to that observed on the as-irradiated Zr-1%Nb alloy [13]. This suggests that both the creep test and the tensile test did not affect significantly the needle precipitates.

On the other hand it turns out that it is very difficult to clearly distinguish dislocation loops after the tensile tests. As shown on Fig. 9 very few loops are clearly observed and in addition

the small loop contrast can be mistaken for the contrast coming from the needle precipitates. This observation has to be compared to the TEM observations described in [2] after post-irradiation creep tests. Indeed, after post-irradiation creep performed at 400°C under a 130 MPa applied stress, small <a> loops could still be observed with size and density in rather good agreement with the microstructure observed after heat treatments at 400°C. This proves that the tensile test performed after the post-irradiation creep test has strongly affected the remaining loops.

It can also be pointed out that the dislocations observed on Fig. 10(a) after tensile tests seem to be pinned on needle-like precipitates and/or on residual <a> loops.

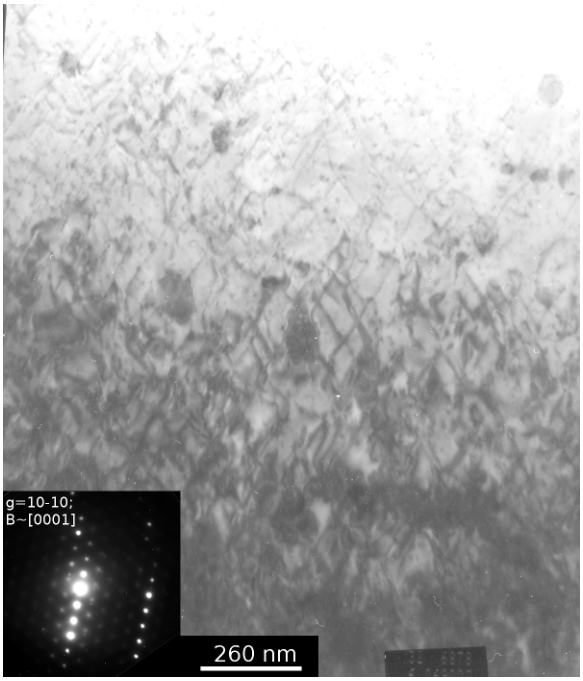

a)

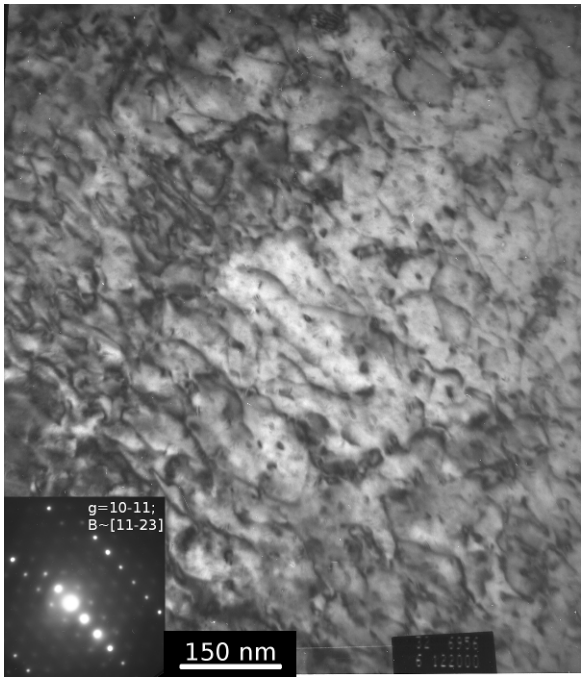

b)

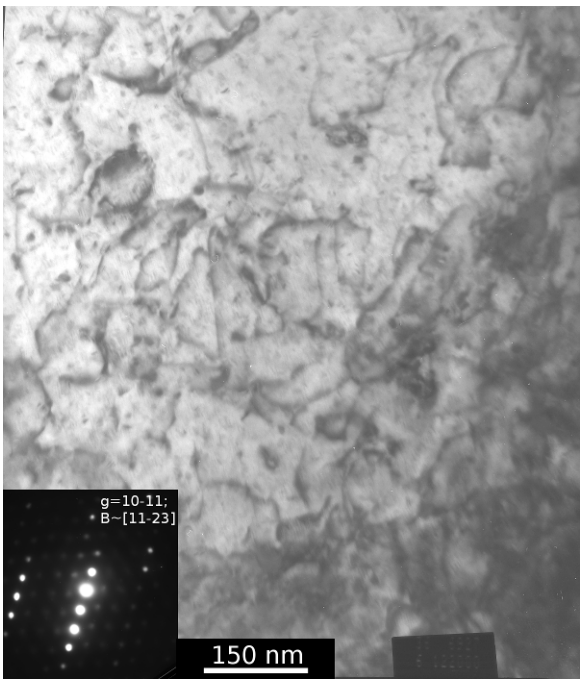

c)

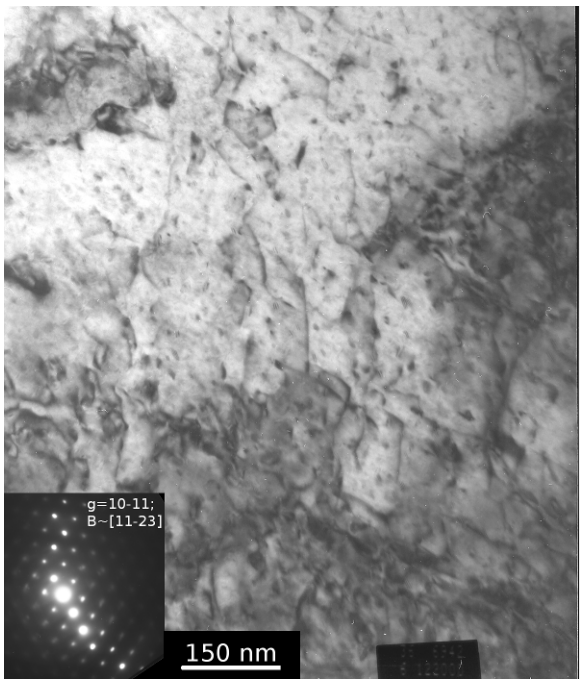

d)

Figure 9: a) and b) Pictures of the ZrNb-2a specimen. c) and d) pictures of the ZrNb-3a specimen. a) dislocations gliding in the prismatic plane observed with the electron beam close to the <c> axis ($B \approx [0001]$) using the diffraction vector $g = 10\bar{1}0$, b) dislocations observed

with the electron beam close to the <c+a> direction ($B \approx [1\,1\bar{2}3]$) using the diffraction vector $g = 10\bar{1}1$, c) dislocations observed with the electron beam close to the <c+a> direction ($B \approx [1\,1\bar{2}3]$) using the diffraction vector $g = 10\bar{1}1$, d) dislocations observed with the electron beam close to the <c+a> direction ($B \approx [1\,1\bar{2}3]$) using the diffraction vector $g = 10\bar{1}1$.

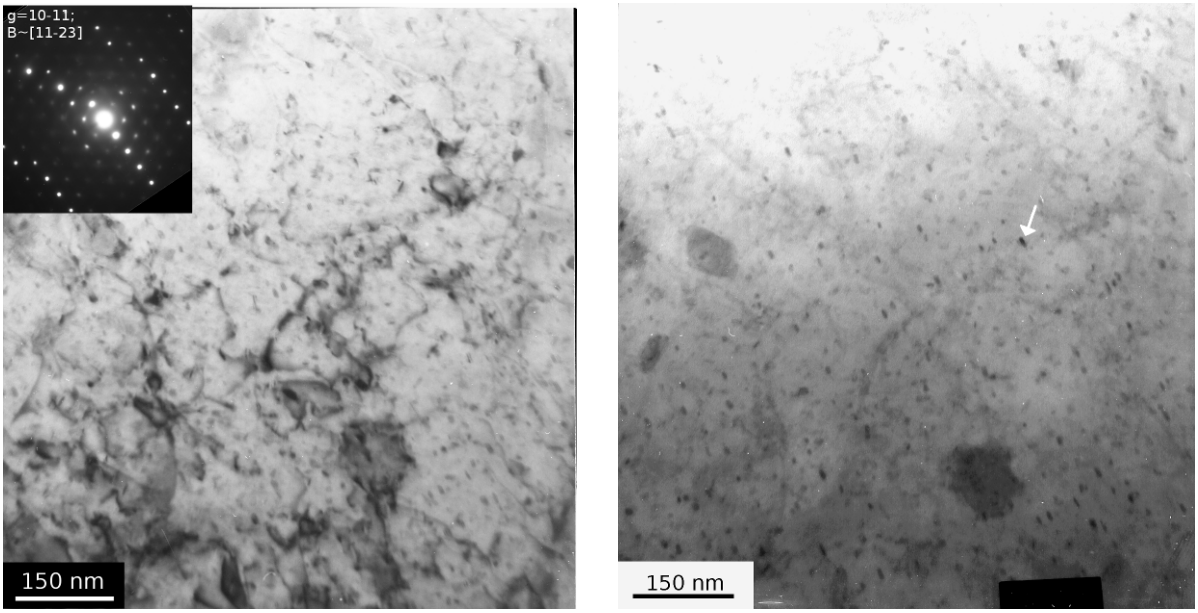

a) b)

Figure 10 : Pictures of the ZrNb-2a specimen. a) dislocations and needle precipitates observed with the electron beam close to the <c+a> direction ($B \approx [1\,1\bar{2}3]$) using the diffraction vector $g = 10\bar{1}1$,b) needle precipitates observed in an out-of-contrast diffraction conditions (no lattice plane is in Bragg diffraction condition). An arrow shows one needle precipitate.

4. Discussion

4.1 Discussion on the behavior of the as-irradiated Zr-1%Nb specimens

The TEM observations have shown that in the as-irradiated Zr-1%Nb there is a very high density of small <a> type dislocation loops induced by irradiation [2]. This very high density of small dislocation loops that act as obstacles against dislocation motion explains the strong irradiation induced hardening measured through tensile and hardness tests.

It has been shown by TEM that the as-irradiated Zr-1%Nb specimen tested at room temperature and interrupted at UTS exhibits dislocation channels. This deformation mechanism consists of the clearing of the irradiation induced loops by gliding dislocations on only one slip system leading to the creation of a defect free zone that becomes a preferred area for further dislocations gliding [8, 9]. This phenomenon leads to the localization of the plastic strain at the grain scale and to a softening at the microscopic scale. This mechanism, as well as the fact that there is only one activated slip system, can explain the early localization of the plastic strain at the specimen scale which leads to the loss of macroscopic ductility observed after irradiation (decrease of the UE value), the failure mode remaining ductile [10] .

Moreover it has been shown that the dislocation channels observed correspond both to the basal and prismatic planes proving that during ring tensile tests these two slip systems can be activated at room temperature. This observation has to be compared with the analysis of the post-irradiation deformation mechanisms at 350°C described in [8, 9]. It has been proven, indeed, throughout many TEM observations that for both transverse tensile tests and internal pressure tests performed at 350°C the deformation occurs by dislocation channeling mechanism. It has also been shown that up to the ultimate tensile strength only basal channeling occurs. Only after the UTS prismatic, pyramidal as well as basal channels are observed on ring specimens tested at 350°C [9]. On the other hand it has been shown that at

350°C when the grains are not properly orientated to allow basal slip, as they are for axial tensile tests, prismatic channels are observed. These deformation mechanisms are very different from the deformation mechanisms observed before irradiation. Before irradiation, indeed, the deformation occurs by the way of an homogeneous gliding of dislocations within the grains mainly by prismatic slip. The change in the principal slip system has been attributed to the difference in junction reactions between the loops and the dislocations gliding in the prismatic plane or the dislocations gliding in the basal plane [8]. Indeed, the irradiation induced loops can be easily swept up by the dislocation gliding in the basal plane since the junctions allow gliding which favors an easy dislocation channeling mechanism in the basal plane. On the other hand the sweeping of loops by dislocations gliding in the prismatic plane is more difficult since the junctions are sessile explaining that the dislocation channeling mechanism in the prismatic plane is more difficult. However, the fact that at room temperature for ring test interrupted at the UTS both basal channels and prismatic channels are observed can be understood if the evolution of the Critical Resolved Shear Stresses (CRSS) of the various slip systems with temperature is taken into account. It has been shown, indeed, by Akthar [11] while testing at high temperature pure zirconium single-crystals that the basal CRSS, which is higher than the prismatic CRSS, decreases quickly as a function of the temperature whereas the prismatic CRSS decreases more slowly. A schematic plot of this evolution is proposed on Fig. 11 for polycrystalline Zr-1%Nb at lower temperatures. On the other hand it has been shown by Onchi [12] that the yield stress of both irradiated and unirradiated recrystallized Zy-2 decreases with the test temperature, the decrease being only slightly slower for the irradiated specimens between 20°C and 300°C. This proves that the test temperature has only a small influence on the irradiation induced hardening. It can therefore be assumed that the evolution of both the basal and prismatic CRSS with irradiation only consists of a constant increment of the CRSS independent of the temperature, the increment of

CRSS being much higher for prismatic slip than for basal slip [8, 13]. As proposed on the schematic plot given in Fig. 11 a reversal of the prismatic and basal CRSS occurs with irradiation at 350°C leading to a change of the easy glide slip system. On the other hand, at 20°C, no reversal of the CRSS occurs but the basal and the prismatic CRSS become very close to each other therefore explaining that both basal and prismatic channels can be observed depending on the grain orientation.

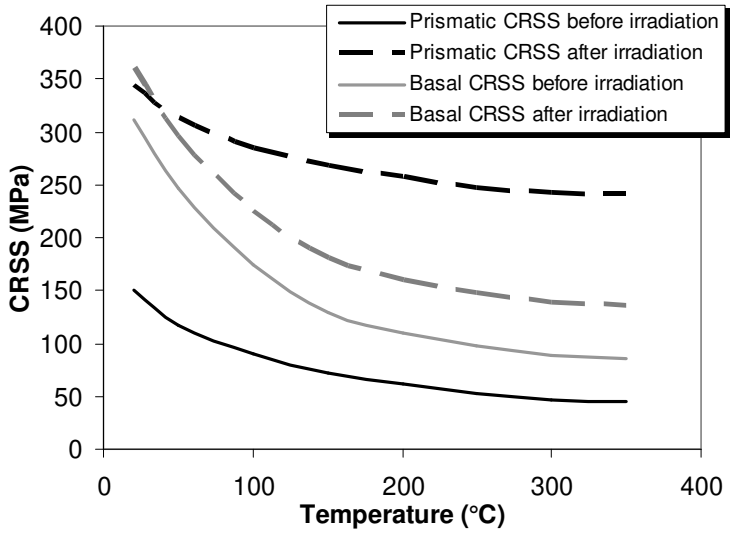

Figure 11: Schematic plot of the evolution of the prismatic and basal CRSS with temperature before and after irradiation.

4.2 Discussion on the behavior of the Zr-1%Nb specimens after post-irradiation creep

It has been shown [2] that during creep tests at 400°C and 450°C an annealing of the radiation induced loops occurs. The annealing of the radiation induced loops explains the recovery of the radiation hardening measured using tensile and hardness tests after post-irradiation creep. However, as shown on Fig. 4 after post-irradiation creep the recovery of the hardening is only partial since the strength (or hardness) remains higher than for the non irradiated material. This phenomenon has several origins. Firstly, after 984 or 3301 hours at 400°C remaining loops can still be present in the material, the loop annealing being slow at this temperature [2,

3]. Secondly, the needle precipitates are also another source of residual hardening. Indeed, even after 960 hours post-irradiation heat treatment performed at 450°C [2], the hardness of the material is still not fully recovered (Fig. 6). In this condition, only very few large loops remain present in the material [2, 3]. These remaining loops cannot explain the residual hardening. The residual hardening is therefore due to the very small precipitates present in very high density in the material after irradiation [14] which can act as obstacles to dislocation motion. These two reasons can explain the residual hardening observed. Nevertheless, as it has been pointed out, after creep performed at 400°C during 984 or 3301 hours, the hardness remains higher than the hardness measured after post-irradiation heat treatment performed at 400°C during 500 hours only. This proves that the residual hardening cannot only be explained by the remaining loops and the needle precipitates that are both present in the case of the heat-treated material.

It has been proven [2] that during creep tests performed at 400°C with an applied stress of 130 MPa in addition to the recovery of the radiation induced loops the microstructure exhibits a high dislocation density, much higher than the dislocation density observed in the non irradiated material for the same creep strain. It has been proposed that this high dislocation density is the result of dislocation multiplication due to the remaining loops that act as obstacles and therefore decrease the dislocation mean free path. The high density of small needle-like precipitates could also increase the dislocation multiplication. This higher dislocation density observed after post-irradiation creep performed at 400°C with an applied stress of 130 MPa could explain the higher residual hardening than after heat treatment.

The TEM observations made after the ring tensile tests following the post-irradiation creep test have shown that the irradiation induced loops seem to have been fully cleared on the contrary of what occurred with the microstructure observed after post-irradiation creep where

remaining loops could still be seen [2]. This can probably be explained by a homogeneous sweeping of loops by gliding dislocations as it is observed within the dislocation channels on the as-irradiated material.

It has been shown that the deformation occurs homogeneously throughout the grain by dislocation glide, no channel being observed. The easy glide system is the prismatic slip system as shown on Fig. 8(a). The deformation mechanisms are therefore similar to the deformation mechanisms occurring for the non irradiated material. This can explain that after post irradiation creep the material recovers its ductility. However, the dislocation density appears to be very high for this plastic strain level (2.43% and 5.16%). The high dislocation density already observed after creep test could explain these observations. Probably additional dislocation multiplication also occurs during the ring tensile test. Indeed, the high dislocation density, the remaining loops and the high density of needle-like precipitates decreases the mean free path along which the dislocations may glide. This could therefore lead to a high dislocation multiplication during the tensile test. This phenomenon could explain that the strain hardening is higher after post-irradiation creep compared to the non irradiated material. The fact that the macroscopic ductility (UE and TE values) of the material remains lower than the macroscopic ductility of the non irradiated material could also be explained by the high dislocation density. Indeed the material is already strain-hardened, like a cold-worked material, its remaining strain hardening capability is therefore reduced.

4.3 Discussion on the behavior of the Zy-4 specimens after post-irradiation creep

It is well known that non irradiated stress-relieved Zy-4 exhibits a higher strength or hardness than non irradiated recrystallized Zr-1%Nb as confirmed by Tables 6 and 7. This can be explained because the two materials show different microstructures. Indeed, Zy-4 is a Stress Relieved alloy with elongated grains that are very small (between 0.1 and 0.5 µm) in the

transverse direction and a very high dislocation density, whereas the Zr-1%Nb alloy is a recrystallized alloy with larger equiaxial grains (5 µm) and very low dislocation density. These two microstructural features can explain the higher strength of the Zy-4. This material exhibits also a lower ductility because of its strain-hardened state and therefore its lower strain-hardening capability.

As for the Zr-1%Nb alloy, strong irradiation induced hardening is also observed for Zy-4, the change in strength (YS and UTS) and hardness being similar for the two materials. Zy-4 specimens have not been observed by TEM in this study. The irradiation hardening can also be explained by the high density of small irradiation induced <a> loops. After post-irradiation creep, the strength and hardness of the Zy-4 are recovered probably due to the annealing of the <a> loops. It has indeed been shown [1] that after 10 days at 470°C, a partial irradiation defects recovery is observed showing a decrease of the number of <a> loops and an increase of their size. Moreover, after creep, the strength (YS and UTS) and microhardness can become lower than the values measured for non irradiated material depending on the creep tests conditions. This phenomenon has already been observed after post-irradiation heat treatment [2]. The fact that the strength or hardness can decrease below their initial non irradiated values is probably due to the recovery of the dislocation network already present before irradiation and maybe to a start of recrystallization. Indeed it has been observed previously [1] that after 10 days post-irradiation heat treatment at 520°C the initial structure has evolved towards a structure of equiaxial grains with a low dislocation density. However, according to Dunlop et al. [15], even after 17071 hours at 400°C the recrystallization might remain very low. The additional softening would be therefore mainly attributed to the annealing of the non irradiated dislocation network. The fact that the effect of post-irradiation creep on Zy-4 is the same as a heat treatment, contrary to Zr-1%Nb, can probably be attributed to the saturation of the dislocation density with plastic strain. Indeed, the dislocation

density is already very high in the material, the increase of the dislocation density during creep is therefore not significant. This also explains that the strain hardening behavior of the specimen after post-irradiation creep is similar to the strain hardening behavior of the non irradiated material.

5. Conclusions

The effect of post-irradiation creep test on the subsequent room temperature mechanical properties of zirconium alloys has been investigated and interpreted in terms of deformation mechanisms observed by TEM. It has been shown that for both stress-relieved Zy-4 and recrystallized Zr-1%Nb alloys post-irradiation creep tests lead to the recovery of the strength of the material (decrease of the YS and UTS values towards its non irradiated values) and to a recovery of the ductility of the material (increase of the UE and TE values towards its non irradiated values). In the case of the Zr-1%Nb it has been proven that the recovery of the strength of the material is due to the irradiation loops annealing that occurs during post-irradiation creep test. It has also been shown that the loss of macroscopic ductility of the as-irradiated material is due to the dislocation channelling mechanism that leads to an early localization of the plastic strain at the specimen scale.

On the other hand, after post-irradiation creep tests followed by a tensile test no channel is observed, the deformation occurring homogeneously throughout the grains, and the deformation mechanisms are similar to that of the non irradiated material. These observations explain the recovery of the strength and ductility after post-irradiation creep. However, the coupling between the recovery of the mechanical properties and the hydrides reorientation has still to be investigated in order to obtain a full understanding of the mechanical behaviour after dry transportation or dry storage.

References

[1] Cappelaere, C., Limon, R., Gilbon, D., Bredel, T., Rabouille, O., Bouffioux, P. and Mardon, J. P. "Impact of Irradiation Defects Annealing on Long-Term Thermal Creep of Irradiated Zircaloy-4 Cladding Tube", *Zirconium in the Nuclear Industry: Thirteenth International Symposium, ASTM STP 1423*, G. D. Moan, and P. Rudling, Eds., ASTM International, West Conshohocken, PA, 2002, pp. 720-739.

[2] Ribis, J., Onimus, F., Béchade, J. L., Doriot, S., Cappelaere, C., Lemaignan, C., Barbu, A., and Rabouille, O.; "Experimental and Modeling Approach of Irradiation Defects Recovery in Zirconium Alloys: Impact of an Applied Stress", *J. ASTM Intl*, Vol. 5, No. 3, ASTM International, 2008, Paper ID JAI101118.

[3] Ribis, J., Onimus, F., Béchade, J. L., Doriot, S., Cappelaere, C., Lemaignan, C. and Barbu, A., "Experimental study and numerical modelling of the irradiation damage recovery in zirconium alloys", submitted to Journal of Nuclear Materials.

[4] Northwood, D.O., London, I.M. and Bahen, L.E., "Elastic constants of zirconium alloys", Journal of Nuclear Materials, Vol. 55, 1975, pp. 299-310.

[5] Torimaru, T., "Changes in Mechanical Properties of Irradiated Zircaloy-2 Fuel Cladding Due to Short Term Annealing," Journal of Nuclear Materials, Vol. 238, 1996, pp. 169-174.

[6] Dollins, C.C., "Post Irradiation Recovery of Irradiation Damage", Radiat. Eff., Vol. 16, 1972, pp. 271-280.

[7] Busby, J.T., Hash, M.C. and Was, G.S., "The relationship between hardness and yield stress in irradiated austenitic and ferritic steels", Journal of Nuclear Materials, Vol. 336, 2005, pp. 267-278.

[8] Onimus, F., Monnet, I., Béchade, J.L., Prioul, C. and Pilvin, P., "A statistical TEM investigation of dislocation channeling mechanism in neutron irradiated zirconium alloys", Journal of Nuclear Materials, Vol. 328, 2004, pp. 165-179.

[9] Onimus, F., Béchade, J.L., Prioul, C., Pilvin, P., Monnet, I., Doriot, S., Verhaeghe, B., Gilbon, D., Robert, L., Legras, L., and Mardon, J.P.; "Plastic Deformation of Irradiated Zirconium Alloys: TEM Investigations and Micro-Mechanical Modeling", *J. ASTM Intl*, Vol. 2, No. 8, ASTM International, 2005, Paper ID JAI12424.

[10] Fregonese, M., Régnard, C., Rouillon, L., Magnin, T., Lefebvre, F. and Lemaignan, C., "Failure mechanisms of irradiated Zr alloys related to PCI: activated slip systems, localised strains, and iodine induced stress corrosion cracking", *Zirconium in the Nuclear Industry: Twelfth International Symposium*, *ASTM STP 1354*, G.P. Sabol, and G.D. Moan, Eds., ASTM International, West Conshohocken, PA, 2000, p. 377.

[11] Akhtar, A., "Basal slip in Zirconium", Acta metallurgica, Vol. 21, 1973, pp. 1-11.

[12] Onchi, T., Kayano, H. and Higashiguchi, Y., "The inhomogeneous deformation behavior of neutron irradiated Zircaloy-2", Journal of Nuclear Materials, Vol. 88, No. 2-3, 1980, pp. 226-235.

[13] Onimus, F. and Béchade, J.L., "A polycrystalline modeling of the mechanical behavior of neutron irradiated zirconium alloys", Journal of Nuclear Materials, Vol. 384, No. 2, 2009, pp. 163-174.

[14] Doriot, S., Gilbon, D., Béchade, J.L., Mathon, M.H., Legras, L., and Mardon, J.P.; "Microstructural Stability of M5™ Alloy Irradiated up to High Neutron Fluences, *J. ASTM Intl*, Vol. 2, No. 7, ASTM International, 2005, Paper ID JAI12332.

[15] Dunlop, J.W.C., Bréchet, Y.J.M., Legras, L. and Zurob, H.S., "Modelling isothermal and non-isothermal recrystallisation kinetics. Application to Zircaloy-4", Journal of Nuclear Materials, Vol. 366, No. 1-2, 2007, pp. 178-186.